ISTITUTO NAZIONALE DI RICERCA METROLOGICA
Repository Istituzionale

Three-Dimensional Photonic Circuits in Rigid and Soft Polymers Tunable by Light

This is the author's accepted version of the contribution published as:

Original
Three-Dimensional Photonic Circuits in Rigid and Soft Polymers Tunable by Light / Nocentini, Sara; Riboli, Francesco; Burresi, Matteo; Martella, Daniele; Parmeggiani, Camilla; Wiersma, Diederik S.. - In: ACS PHOTONICS. - ISSN 2330-4022. - 5:8(2018), pp. 3222-3230. [10.1021/acsphotonics.8b00461]

Availability:
This version is available at: 11696/66831 since: 2021-02-19T18:38:13Z

Publisher:
AMER CHEMICAL SOC

Published
DOI:10.1021/acsphotonics.8b00461

Terms of use:
Visibile a tutti

This article is made available under terms and conditions as specified in the corresponding bibliographic description in the repository

Publisher copyright
American Chemical Society (ACS)
Copyright © American Chemical Society (after peer review and after technical editing by the publisher)

(Article begins on next page)

19 October 2021

Three dimensional photonic circuits in rigid and soft polymers tunable by light

Sara Nocentini[*1], Francesco Riboli[1,2], Matteo Burresi[1†], Daniele Martella[1,2,3], Camilla Parmeggiani[1,2,3] and Diederik S. Wiersma*[*1,4]*

[1] *European Laboratory for Non Linear Spectroscopy, via N. Carrara 1, Sesto Fiorentino, Firenze 50019, Italy*

E-mail: nocentini@lens.unifi.it, wiersma@lens.unifi.it

[2] *CNR-INO Sesto Fiorentino, Via Madonna del Piano 10, Firenze 50019, Italy*

[3]*Chemistry Department "Ugo Schiff", University of Florence, Via della Lastruccia 3, Sesto Fiorentino, Firenze 50019, Italy*

[4] *Physics Department, University of Florence, via G. Sansone 1, Sesto Fiorentino, Firenze 50019, Italy*

[†] Now at *Leonardo Company, Via delle Officine Galileo, 1, Campi Bisenzio, Firenze 50013, Italy*

Keywords: polymer photonics, 3D integrated photonic circuits, tunable whispering gallery mode resonators, direct laser writing, liquid crystalline networks

Abstract

Polymeric matrices offer a wide and powerful platform for integrated photonics, alternative to the well-established silicon photonics technology. The possibility to integrate, on the same chip, different customized materials allows for many functionalities, like the possibility to dynamically control the spectral properties of single optical components. Within this context, this article reports on the fabrication and optical characterization of integrated photonic circuits for the telecom C-band, made of a combination of both rigid and tunable elastic polymers. By using a 3D photolithographic technique (direct laser writing), in a single step process, every building block of the polymeric circuit is fabricated: straight and bent waveguides, grating couplers, and single and vertically coupled whispering gallery mode resonators with high Q-factor designed in planar and vertical geometries. Using this platform, a new type of operation was introduced through true three dimensional integration of tunable photonic components, made by liquid crystalline networks that can be actuated and controlled by a remote and non-invasive light stimulus. Depending on the architecture, it is possible to integrate them as elastic actuators or as constituents of the photonic cavity itself. The two strategies then exploit the optical induced deformation and variation of its refractive index, inducing a net red or blue shift of the cavity resonances, respectively. This work paves the way for light tunable optical networks that combine different photonic components and glassy and shape-changing materials in order to implement further photonic circuit requirements.

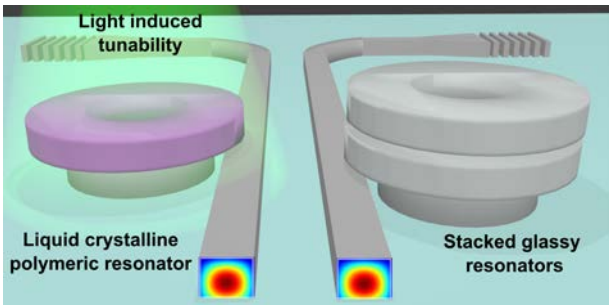

Introduction

Integrated photonic circuits combine single photonic components to perform light manipulation on a single chip. Guiding light and processing the carried optical information increase the potential of integrated electronics, solving some of its intrinsic limitation such as speed and bandwidth needed in telecommunication and optical signal processing.[1] While the silicon technology still represents the reference platform of integrated photonic circuits,[2,3] polymeric materials allow for integration of both active and passive optical components on several flexible and rigid substrates.[4] Compared to inorganic materials, the outstanding characteristic of polymeric materials relies on the possibility to control their chemical and physical properties by chemically modifying the structure of the constituent monomer or the functional groups, while a material functionalization (as stimuli responsiveness) can be addressed through selective doping or reactions. Such chemically engineered polymers indicate the potential of this technology to be a cost-effective (respect to semiconductors) and customizable solution to the production of high-differentiated performance in integrated optical circuitry. Polymers can be patterned through different lithographic techniques also combining diverse materials into the same platform to address different functionalities, implementation that results complementary to silicon technology depending on the desired application.

The standard fabrication techniques for photonic circuits, as UV lithography and e-beam lithography, are based on a planar structuration (resolution up to sub-10 nm features[5,6]). The exploitation of the third dimension - orthogonal to the planar substrate - represents a difficult task, but improves the potential for integration, permitting even more complex light manipulation as polarization control[7,8] or device tunability[9] and, more in general, achieving denser integrated optical networks.[10] Previous works based on multi-step procedures of planar lithography alternated with sacrificial intermediate layer depositions, have been demonstrated to implement circuit three-dimensionality.[11-13] However, these procedures rely on repeated alignment procedures and material depositions, requiring several fabrication iterations to reach the desired vertical structure stack.

To overcome issues on material properties and fabrication restrictions, and in order to have more design freedom, we propose a simpler, mask-free approach to fabricate high-quality three-dimensional integrated photonic circuits made of polymeric materials. The direct laser writing (DLW) technique, in a single writing step, allows to take full advantage of the third dimension, while the vast selection of polymers with their broad range of properties permits functionalization of each single building block of the photonic circuit, paving the way for the realization of a three-dimensional active and tunable polymeric integrated network.

The working principle of direct laser writing, (a two-photon absorption polymerization process on monomeric mixtures[14]), allows to overcome certain limitations of planar technology. Recent examples range from photonic components,[15] to biological scaffolds,[16] microfluidics,[17] and micromechanics.[18] M. Shumann et al.[19] realized hybrid 2D-3D optical devices for integrated optics, by combining a silicon nitride circuit previously patterned with e-beam lithography, with a suspended waveguide and a whispering gallery mode resonator (WGMR) realized by DLW. This 3D patterning procedure showed low cavity quality factors and no control over the disk-waveguide coupling was achieved. Other polymeric resonators, both active and passive high quality factor cavities[20,21,21A] have been fabricated by DLW but their integration into a photonic circuit, to the best of our knowledge, is still missing. In fact, many are the critical aspects in the waveguide-cavity coupling that limit their fabrication and applicability. On the other hand, the possibility offered by DLW to integrate different photopolymerizable materials enables to combine glassy and elastic soft polymers on the same chip.[22] Liquid crystalline networks (LCN) are smart elastomers that show liquid crystalline phases within a crosslinked elastic network whose properties such as shape-change and birefringence can be driven by different external stimuli, among them, light.[23,24] The reshaping property of LCN, usually employed in mimicking muscle functionality in robotics,[25,26] can be differently exploited in photonics in order to deform and then tune optical properties of photonic structures. Elasticity of photo-responsive optical devices enlarges the potentiality of integrated circuits providing solution to the open demand of tunability of their photonic properties. Interesting examples of rigid polymeric high quality factor cavities have been integrated on flexible and elastic substrate enabling a mechanical deformation of the elastic substrate that enables in their optical property control.[22A,B] Tunability has also been previously addressed in whispering gallery mode cavities exploiting refractive index variation through electro-optic effect,[27-27A] thermo-optic tuning,[28-28D] free carrier injection in silicon photonics[29] or the employ of liquid crystals.[30] The proposed strategies demonstrate fine[27-27A,30] and wide[28-28D] resonant wavelength scans (up to 12 nm in racetrack ring resonators, Q=8000) achieved by a low tuning power of 21 mW per free spectral range.[28D] Hence we demonstrate the integration in a polymeric photonic circuit of high quality factor vertically-coupled cavities, in a fully three dimension geometry. Furthermore, in order to implement optically controlled photonic properties, high quality factor whispering gallery mode resonators are tuned by light in two different fashions: exploiting a LCN actuator placed on the top of the cavity and fabricating the resonator directly in the photo-responsive LCN matrix. With an alternative method for dielectric platform, based on a remote optical control of photo-responsive smart materials, competitive actuation power and tuning range are here demonstrated. Moreover the local optical activation of polymeric structures on dielectric substrates reduces the issue of thermal cross-talk in silicon circuitry platforms. We propose light activated tuning of polymeric photonic circuit elements that allows to reproduce the already achieved results in silicon photonics using cheaper materials and simpler fabrication and opening at the same time to add further functionalities on the same dielectric chip.

Result and Discussion

PASSIVE RIGID PHOTONIC COMPONENTS

In this work, polymeric integrated structures for light transport and manipulation for telecom C-band, such as straight and bend waveguides, grating couplers, single and vertically coupled WGMRs, were fabricated by DLW (by Nanoscribe GmbH) on a low refractive index substrate (fused silica, n=1.44 @ 1550 nm) taking advantage of the Dip-in configuration (see Methods).[31] Figure 1a shows the scanning electron microscopy (SEM) image of typical building blocks of an integrated optical circuit, such as a single mode 90 degree bent waveguide ended by two grating couplers (input and output). This coupling configuration enables to pass from free space optics to an on-chip light propagation with a contact free characterization of the system. Figure 1b reports the intensity profile of the fundamental TM (dominant polarization vector along *y* axis) and TE (dominant polarization vector along *x* axis) modes of the rectangular waveguides with effective refractive indexes of n_{TM}=1.494 and n_{TE}=1.493 respectively. The waveguide has a bent geometry (30 µm curvature radius), in order to purify the coupled light from the straight and scattered light by selectively filtering the measured signal with a cross polarization configuration. The gratings at the ends of each curved waveguide allow the outcoupling and the detection of light (Figure 1c). The width of the grating is larger than the waveguide in order to collect the whole focalized beam spot and through an in-plane tapered section, the light is conveyed to the single-mode waveguide.

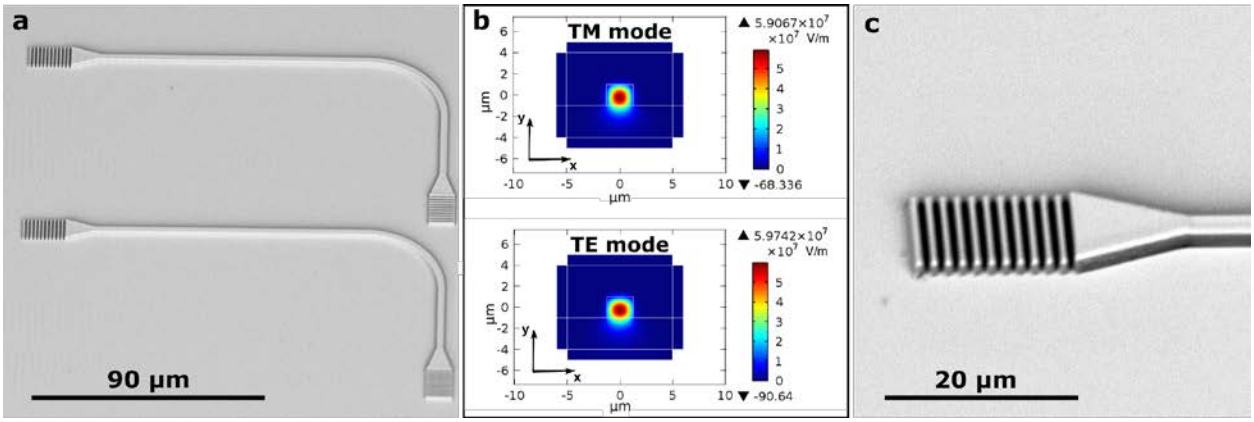

Figure 1: Polymeric waveguides. a) SEM image of two replica of the same integrated optical device. Each device is composed by a waveguide whose structural parameters have been optimized to show monomodal behaviour around 1550 nm. The coupling of light into the waveguide is assured by two grating couplers. b) Intensity profile of the fundamental TM and TE modes. The mode analysis calculation results were obtained with perfect matching layers (pml) around the computation cell. The design and the optimization of the structural parameters of the monomodal waveguide and of the grating coupler have been performed with a finite method based (FEM) commercial software (Comsol Multiphysics). The waveguide has a transversal section of 2 µm (thick) and 2.5 µm (wide). c) Detailed view of the grating coupler. In order to maximize the coupling efficiency, the width of the coupler is larger than of the waveguides to which is connected through a tapered section.

The numerical optimization of the grating shows coupling efficiency at normal incidence (90° coupling geometry) around 3% (around 1500 nm), as expected for structures with a low refractive index contrast.[19] Calculated spectral efficiency for a single grating coupler and their comparison with the experimental results are reported in Supplementary Information (Figure S1). Optimized coupling efficiency can be obtained by tilting the incident input beam of about 10° with respect to the normal direction[32] or by geometrical improvements such as a variable groove depth or apodized geometries[33] or by the employ of gold mirrors[34] or distributed Bragg

reflectors (DBR)[35,36] to reflect upwards the light radiating towards the substrate. Other coupling geometries using 3D horn coupler or arc waveguides can also be adopted, taking advantage of the 3D fabrication, in order to outperform the coupling efficiencies and remove the spectral efficiency dependence.[36A] The grating couplers in micro photonic circuits introduce then insertion losses that dominates the waveguide propagation losses.[19,36B] Waveguide propagation losses are determined by the sum of material absorption losses (typical two photon polymerizable resists have 0.5 dB/cm to 3 dB/cm absorption losses),[36B] substrate leakage losses (negligible for the good confinement factor of 89% and 91% for the TE and TM mode respectively) and scattering losses at sidewall roughness. In our polymeric waveguides, intensity variation related to propagation losses - typical propagation losses are few dB/cm (0.68 dB mm^{-1}) [36A] - are not detectable within our photonic system since they are dominated by insertion losses. The realized waveguides are then used as bus-waveguides to couple light into high quality factor cavities known as whispering gallery mode resonators (WGMRs).[37] The waveguide is lying on the substrate while the WGMR is realized in a suspended geometry in order to increase the modal confinement of the resonant mode and its intrinsic quality factor. This configuration provides for a vertical coupling between guide and resonator without reducing the mechanical stability of the optical circuit. Indeed, if suspended structures - both the waveguide and the ring resonator held by pedestals - are employed, they result highly unstable and difficult to align. Moreover the mutual distance between waveguide and ring for the optimal coupling, critical and sensitive parameter to fabrication fluctuations,[37] reveals to be hard to control also during the development process since electrostatic forces can make the structures collapsing together.[38] Even the use of solvent drying into a critical point dryer does not solve this issue either.[19] In the proposed geometry, the cavity and the waveguide lay in different planes determining an oscillating effective coupling as a function of vertical gap with alternating under- and over-coupling regions, separated by several critical coupling points.[39,40] The structures realized with DLW in a single lithographic step feature then less critical coupling conditions and a mechanically stable vertical coupling between the waveguide and the suspended free-standing ring resonator.[41] Figure 2a shows the three-dimensional rendering of the waveguide and resonator and the entire fabricated system (top view) is imaged by SEM in Figure 2b. The inset of figure 2b displays the intensity distribution in a vertical plane (perpendicular to the substrate) of TM resonant mode circulating in the ring. For the inspected vertical geometry, the coupling efficiency favors the waveguide-to-ring coupling of TM modes that we verified by numerical calculations. The experimental setup has been optimized to detect such polarization component. In these 3D systems, the vertical as well as the lateral displacement between the waveguide and the ring plays a determinant role in the optimal evanescent coupling. For the considered system, the optimal geometry is shown in Figure 2c, where the lateral displacement between the waveguide and the ring, that maximizes the vertical alignment between the eigenmodes of the two structures, can be appreciated. However, different structures can be designed by varying both the lateral and the vertical distance obtaining photonic circuits with different waveguide-to-ring coupling and ring quality factors that can be matched with different applications.

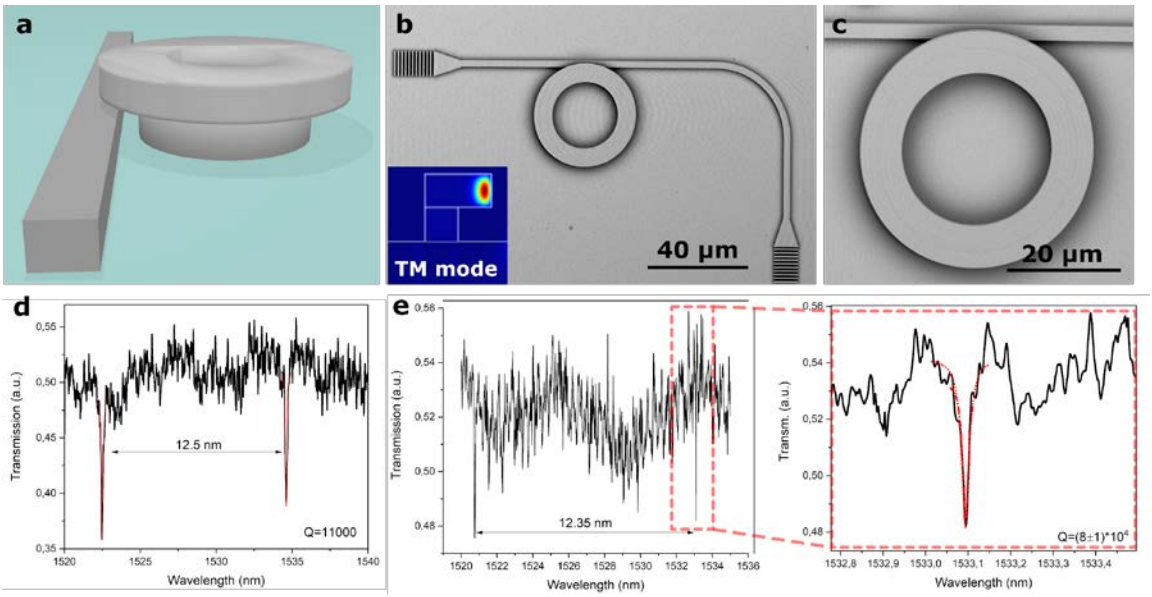

Figure 2: Vertical coupling of polymeric structures. a) Rendering image of a single mode waveguide vertically coupled to a ring resonator. b) SEM image (top view) of the bent waveguide and the whispering gallery mode resonator. The width of the ring is 6 µm with an external radius of 20 µm and a thickness of 2 µm. In the inset, the field intensity map of a TM resonant mode obtained with an axial symmetric mode analysis calculation performed by Comsol Multiphysics. c) Enlarged image of the cavity that shows the lateral displacement between the waveguide and ring in order to maximize the evanescent coupling. d) Typical transmission spectrum of a ring resonator (Q=11000). e) Transmission spectrum of a high quality factor cavity (Q= (8+/-1)*10^4). On the right, the transmission deep detail with its Lorentzian fit.

To characterize the WGM resonators, we performed typical waveguide transmission measurement at telecom wavelengths. The spectrum shown in Figure 2d reveals the characteristic deeps of a high quality factor cavity (with a Q value of 11000). The free spectral range (FSR) is 12.5 nm and the extrapolated effective refractive index of the resonant mode is then n_{eff} = 1.52. The Q-factor is evaluated by fitting the sharp dips (Figure 2e) in the transmission spectrum with a Lorentzian line-shape, obtaining, for higher quality factor resonators, Q=80000. The intrinsic quality factor of whispering gallery mode resonators is determined by different factor: intrinsic material absorption, scattering losses (both intrinsic, as well as generated from the surface), surface absorption losses (e.g. due to the presence of adsorbing compounds), whispering gallery loss (or tunnel loss) related to incomplete total internal reflection at the curved interface. Due to negligible absorption of the polymeric resist at telecom wavelengths, and a radius choice that not limit the quality factor for tunnel losses, intrinsic Q factor values are ruled by the surface scattering losses experienced by the field tail not tightly confined inside the dielectric medium.[41A] The FSR and the effective index n_{eff} of the resonant mode are in good agreement with numerical calculations. On the other hand, the numerical estimated quality Q factor does not provide a value to be compared with the experimental one, since calculations do not take into account possible losses introduced by the imperfections of the cavity surface (such as surface roughness or more in general intrinsic losses) but only the losses associated by the input/output coupling (external losses).

The device, composed by a single WGM resonator vertically coupled to the waveguide, represents a simple three-dimensional device. In order to exploit to its best the versatility of the DLW technique and thus to increase the level of integration in the third dimension, a device composed of two vertically stacked cavities coupled to a input/output bus-waveguide laying on the substrate was explored.

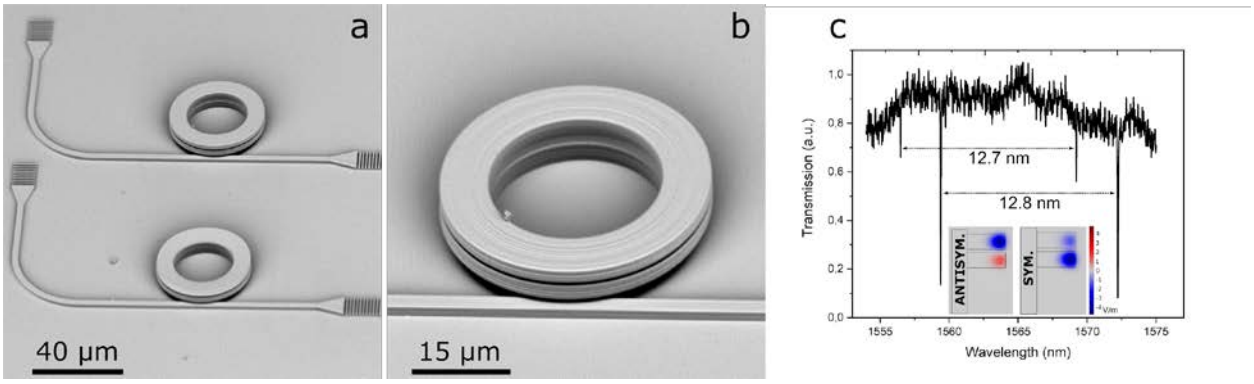

Figure 3: Vertically coupled WGM resonators. a) SEM image (45 degree view) of the waveguide coupled to two vertically coupled WGM resonators. b) Detail of the coupling region. c) Measured transmission spectrum of the waveguide coupled to the two vertically coupled ring resonators. The dip pair corresponds to the symmetric and antisymmetric mode of the two coupled cavities. The inset shows the electric field distribution of the two resonant modes calculated by an axial symmetric calculation (Comsol Multiphysics).

The fabricated structures are reported in Figure 3a. Within the same lithographic procedure, another additional critical parameter is added: the relative distance between the two WGM resonators which in turn determines their coupling strength. Due to the mode spatial confinement into the two polymeric resonators, a shorter relative distance between the two rings with respect to the waveguide-ring separation allows to overlap their evanescent tails creating a double coupled cavity configuration (Figure 3b). Figure 3c shows the spectral response of vertically coupled WGMRs: the wavelength spectrum is characterized by two pairs of dips, with comparable width and spectral separation but different coupling efficiency with the input waveguide mode. They correspond to the symmetric (S) and anti-symmetric (AS) modes of the coupled resonators. Numerical FEM calculations confirm that for each couple of resonances the lowest energy dip is associated to a vertically symmetric field distributions, as expected. The computed effective refractive indexes for the S and AS modes are respectively 1.524 and 1.530 in good agreement with the measured FSR of the S and AS mode resonances.

LIGHT DRIVEN TUNABLE RESONATORS

We demonstrated that exploiting commercial polymers and DLW is possible to realize three-dimensional photonic circuit architectures. However, one of the most relevant advantages of such lithographic technique is the opportunity to combine different polymers (active or passive materials) in the same photonic structure, opening for a controlled and dynamical tuning of its optical response.

In order to realize tunable photonic cavities, we integrate in the photonic circuit a light-driven shape-changing material as liquid crystal networks (LCNs). The main feature of LCN is to reversibly change their shape, in response to an external stimulus, thanks to the molecular organization into liquid crystalline (LC) phases and to the elasticity of the crosslinking network.[42,43] Moreover the deformation can be designed depending on the liquid crystalline molecular

alignment.[44,45] The considered mixture has been chemically engineered in order to be patterned with the DLW[46] and the chemical introduction of an azo-dye, that works as a microscale heater, allows a light induced control over shape deformation of the photonic structure through a local, remote and non-invasive stimulus. To achieve light driven tunability via the activation of the LCN structures, we used a control green laser that matches the azo-dye absorption (maximum at λ = 540 nm) focalized on the photoresponsive structures. The time response of microstructured LCN under a periodic illumination (50 Hz) is in the millisecond time scale.[45] The optically induced rearrangement of LCN polymeric chains - depending on the LC phases - induces also a variation of the refractive index, reversibly losing its birefringent characteristic in favor of a more isotropic phase. These two effects, the shape change and the refractive index variation, are here exploited within two different strategies in order to tune the photonic cavity. In the first case, LCNs are integrated on the top (central part) of Ip-Dip ring resonator (see figure 4a-b) as an elastic cylindrical actuator.[47] Their alignment has been chosen parallel to the cylinder axis so that, once actuated, the structure contracts of the 20% of its total height, h=20 μm, and expands in the perpendicular plane preserving the overall volume unchanged.[45] This architecture allows for a small, gentle and reversible deformation of the Ip-Dip resonator when the LCN are activated via the light stimulus, thanks to the tangent pressure that the LCN actuator impresses on the underlying cavity. The variation of the LCN refractive index does not perturb the guiding properties of the resonator, since the spatial overlap between the LCN structure and the resonant guided mode is negligible. In fact, the spectral characterization of the circuit before and after the integration of the LCN cylinder reveals unperturbed optical properties without any degradation of the quality factor (see Supporting Information, Figure S2). The net result is therefore a small well controlled mechanical deformation that reflects in the spectral red shift (figure 4b) of the resonant wavelength (red round points in Figure 4e) creating a tunable filtering effect. The overall positive shift is 11.5 nm (continuous green line spectrum in Figure 4b) when the light actuation power increases up to 25 mW. The small deformation slightly affects the quality factor value preserving also the dip transmission contrast. A quenching of the resonance red shift is attributed to the refractive index change of the Ip-Dip polymer due to thermo-optical effect that we experimentally estimated in $\Delta\lambda$ =-1.7 nm for an actuation power of 16 mW (see Supporting Information, Figure S3). Considering both effects, the stretching of the cavity radius can be estimated around 170 nm. In the second case, we followed a different approach aiming to maximize light matter interaction between the resonant guided mode and LCN polymers. This second strategy foresees WGM resonators directly fabricated within the LCN matrix in such a way to exploit also the LCN refractive index variation to tune the resonant wavelength. Figure 4c-d show the photonic architecture with its typical transmission spectrum. Liquid crystalline elastomeric WGM resonators with good quality factor (Q=15000) integrated in a simple photonic circuit are demonstrated for the first time. By illuminating LCNs, the extraordinary refractive index, parallel to the cavity symmetry axis, decreases as a function of the control power, while the ordinary refractive index, in the perpendicular plane, slightly increases.[48] This optical modification sums up to the ring mechanical reshaping. Considering then the TM whispering gallery mode, the resonant wavelength is affected by the LCN extraordinary component of the refractive index that under the green laser stimulus shows a variation of $\Delta n = 0.02$ (passing from the nematic to the quasi nematic state[48]) that corresponds to a calculated blue shift of 20 nm. This is not the only contribute to the spectral tuning. In fact, the mechanical expansion of the LCN ring introduces an opposite

red shift. The combination of such effects results in a net blue spectral shift for LCN cavities (Figure 4e, blue triangle and black squared points). From the experimental data, we can retrieve that the resonance tuning as a function of the green laser power is dominated by the refractive index variation. We report the spectral tuning both for Q=15000 and Q=680 quality factor cavities showing that, within this LCN cavity based strategy, the light induced blue shift depends on the optical quality (in terms of intrinsic and extrinsic losses) of the resonator.

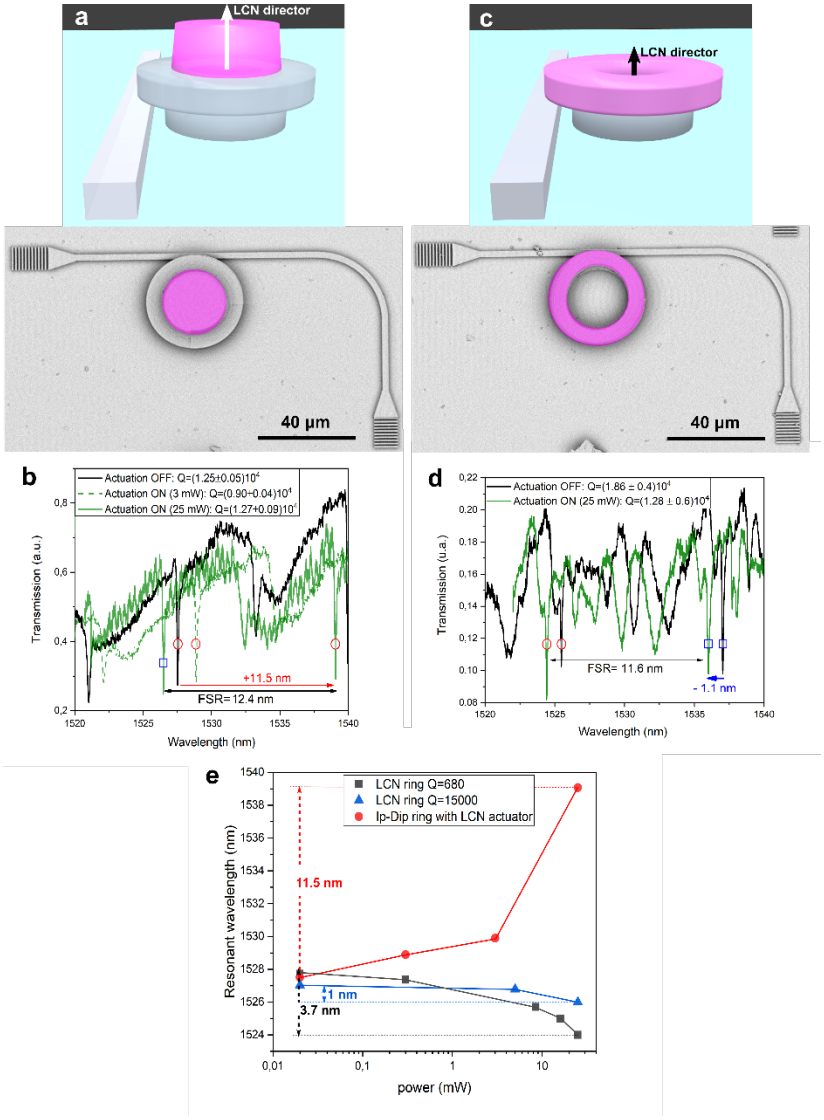

Figure 4: Tunability of a WGM resonator by LCN. Two possible strategies to achieve tunability: in the first column, LCNs are employed as an actuator, in the second column LCNs constitute the cavity itself. a) Rendering, SEM image (top view, false color for the LCN element) and b) transmission spectrum of the waveguide coupled to Ip-Dip WGM resonator. The LCN actuator is placed on the top of the cavity allowing, under proper excitation, to deform the resonator beneath. The quality factor of the resonant mode (Q=12000) is not degraded by the presence of the LCN cylinder. The black line spectrum is recorded with no activation of the LCN actuator, while the green ones correspond to two different activation powers that generate a resonance red shift. c) Rendering, SEM image (top view, false color for the LCN element) and d) transmission spectrum of the waveguide coupled to LCN ring resonator. The FSR is slightly smaller than for the Ip-Dip cavity because of a reduced cavity radius consequence of higher shrinking of the soft material

during the development process. The black line spectrum is recorded without any activation of the LCN cavity, while the green one corresponds to the light activated blue shift of the resonance. e) Tuning of resonant wavelengths for the two different strategies: the red shift of the resonance can be attained when the LCN cylinder is superimposed to the cavity, whereas the blue shift can be achieved in the case of a LCN ring resonator. The error of the central wavelength of the dips extrapolated from the Lorentzian fit is smaller than the plot scatterer size.

Conclusions

Truly three dimensional photonic circuits in different polymeric materials have been integrated on a dielectric platform through the photolithographic technique of direct laser writing.

We designed, fabricated and characterized the typical fundamental building blocks of integrated polymeric photonic circuits as waveguides, grating couplers and high quality factor ring resonators in a dense vertical geometry. Good optical properties have been demonstrated for the configuration of a ring resonator vertically coupled to a bus waveguide, and two vertically-coupled stacked cavities. Further exploiting the possibility to combine different materials by our lithographic technique, we managed to integrate liquid crystalline polymers (LCN) into the photonic circuit and create optically tunable structures. By using photo-responsive deformable materials we control the spectral response of high quality factor whispering gallery mode resonators through a remote, locally focused, non-invasive, optical stimulus.

Tunability has been obtained following two different strategies: in one case a liquid crystalline elastomer is used as a mechanical actuator that slightly and finely changes the shape of polymeric whispering gallery mode resonators, while in the second case the elastomer is used as the photonic material to fabricate the resonator itself. We demonstrate indeed soft ring resonators with quality factor of 15000 that have been realized exploiting a sufficient polymer rigidity to be patterned in suspended designs still preserving its typical elasticity. By following the two different strategies, the spectral response of the photonic circuit can be tuned towards higher or lower energies in a gentle and reversible way. This work represents an important step in the field of tunable optical circuits, combining different photonic components and materials with a spatial and temporal light modulation of photo-responsive cavities. Interestingly, light induced tunability of photo-responsive cavities opens to self-tuning resonators that can accordingly lock their resonance to a fixed wavelength.

Methods

Direct laser writing (DLW): Rigid photonic components. This lithographic technique is based on two-photon absorption polymerization. The non-linear process guarantees a sub-diffraction limited resolution determined by the unitary polymerizable ellipsoid (voxel, volume pixel) with typical minor and major axis respectively of 120 nm and 250 nm. The point by point two-photon absorption polymerization combined with 3D sample piezoelectric movement allows to obtain three-dimensional arbitrary shapes in a single lithographic process. In this work, the Dip-In configuration, has been employed. Within this approach, the femtosecond high power laser (780 nm, 50 MHz) is focused by an immersion high numerical aperture objective directly in a resist drop. The liquid resin (Ip-Dip, after polymerization n= 1.53 @1550 nm[49]), in this case, works both as immersion index matching medium and as photosensitive mixture making the technique

independent on the substrate material.[20] The remaining unpolymerized liquid resist is then removed by organic solvent development in PGMEA (propylene glycol methyl ether acetate) and isopropanol. The chosen mixture that matches the Dip-in DLW configuration is the commercial resist, Ip-Dip (Nanoscribe GmbH). Thanks to the refractive index contrast between the polymer (n= 1.53 @1550 nm [17]) and the fused silica glass is possible to well confine light even in planar structures directly lying on the substrate. **Soft photonic elements.** The same lithographic technique is exploited to fabricate the soft elastic components in a second step process. The fabrication of LCN elements combined to a rigid polymeric structure has been obtained in a two-step DLW process as clear demonstration of how structures made of different materials can be polymerized and vertically aligned on the same substrate. Ip-Dip has been firstly patterned to create the rigid parts of the circuit. Then the unpolymerized mixture has been removed by a chemical development procedure and a glass cell to control the molecular LC alignment has been built around the fabricated structure. The mixture keeps the nematic phase at room temperature for many hours and within the polymerization process the molecular alignment is freezed inside the patterned structure. Into the second fabrication step, the polymerization of LCN was performed. The mesogen alignment was selected parallel to the LCN component symmetry axis so that, once stimulated, the structure contracts along the director and expands in the orthogonal plane.

Alignment control of the LCN mixture

To control the liquid crystalline alignment we take advantage of coated glass cells. To obtain an homeotropic alignment, in fact, we employ both the silica substrate and the cell upper glass, previously covered (by spin coating) with a thin sacrificial layer of polyimide that induce a liquid crystalline molecular vertical alignment. 10 µm spheres were used a spacer in between the two glasses. The LCN mixture was then infiltrated inside the cell at 70 ° (isotropic phase) and then cooled down to the nematic phase at 45°. Before starting the cavity writing procedure, the LC alignment inside the cell is checked with a polarized microscope. To guarantee the vertical alignment of the cavity on its pedestal and of the actuator on the ring, a calibrated system of coordinates respect to the center of the ring was chosen in the lithographic process.

Experimental apparatus

The experimental apparatus employed for the optical characterization of the polymeric photonic circuits consists of a standard transmission setup. The optical signal is coupled to the photonic circuit by focusing the input beam with a 10X objective (Mitutoyo Plan NIR) on the input coupler. The output signal is then collected with a 4X objective in whose conjugate plane we placed a pinhole in order to spatially filter only the light transmitted by the output grating. To further clean the transmitted signal from spurious signals (i.e. straight light, that can pass through the pinhole but has not propagated in the photonic circuit) we placed a second polarizer, in a cross-polarization configuration with respect to the input one, between the pinhole and the detector. The spectral circuit properties are retrieved exploiting a NIR tunable laser source with scanning resolution of 1 pm and a photodiode detector. To maximize the signal to noise ratio of the transmitted signal we modulate the input signal with a lock-in amplifier. The transmission spectrum of the photonic circuit is retrieved by deconvoluting the transmitted light from the lock-in modulation.

SUPPLEMENTARY MATERIAL

See Supplementary material for the complete technical discussion and experimental details.

Acknowledgements

The research leading to these results has received funding from the European Research Council under the European Union's Seventh Framework Program (FP7/2007–2013)/ERC grant agreement n [291349] on photonic micro robotics and Laserlab-Europe, H2020 EC-GA 654148; and from Ente Cassa di Risparmio di Firenze (2015/0781).

Bibliography

1 Kirchain, R.; Kimerling, L. A roadmap for nanophotonics. *Nat. Photonics* **2007**, *1*(6), 303.

2 Leuthold, J.; Koos, C.; Freude, W. Nonlinear silicon photonics. *Nat. Photonics* **2010**, *4*(8), 535.

3 Soref, R. The past, present, and future of silicon photonics. *IEEE J. Sel. Top. Quantum Electron.* **2006**, *12*(6),1678-1687.

4 Ma, H.; Jen, A.Y.; Dalton, L.R. Polymer-based optical waveguides: materials, processing, and devices. *Adv. Mater.* **2002**, *14*(19), 1339-1365.

5 Manfrinato, V.R.; Stein, A.; Zhang, L.; Nam, C.Y.; Yager, K.G.; Stach, E.A.; Black, C.T.; Aberration-Corrected Electron Beam Lithography at the One Nanometer Length Scale. *Nano Lett.* **2017**, *17*(8), 4562-4567.

6 Li, L.; Liu, X.; Pal, S.; Wang, S.; Ober, C.K.; Giannelis, E.P. Extreme ultraviolet resist materials for sub-7 nm patterning. *Chem. Soc. Rev.* **2017**, *46*(16), 4855-4866.

7 Watts, M.R.; Haus, H.A. Integrated mode-evolution-based polarization rotators. *Opt. Lett.* **2005**, *30*(2), 138-140.

8 Zhang, J.; Yu, M.; Lo, G.Q.; Kwong, D.L. Silicon-waveguide-based mode evolution polarization rotator. *IEEE J. Sel. Top. Quantum Electron.* **2010**, *16*(1), 53-60.

9 Li, M.; Pernice, W.H.P.; Tang, H.X. Tunable bipolar optical interactions between guided lightwaves. *Nat. Photonics* **2009**, *3*(8), 464.

10 Topol, A.W.; La Tulipe, D.C.; Shi, L.; Frank, D.J.; Bernstein, K.; Steen, S.E.; Kumar, A.; Singco, G.U.; Young, A.M.; Guarini, K.W.; Ieong, M.. Three-dimensional integrated circuits. *IBM J Res Dev.* **2006**, *50*(4.5), 491-506.

11 Ramiro-Manzano, F.; Prtljaga, N.; Pavesi, L.; Pucker, G.; Ghulinyan, M.. A fully integrated high-Q whispering-gallery wedge resonator. *Opt. Express* **2012**, *20*(20), 22934-22942.

12 Fang, Z.; Yao, N.; Wang, M.; Lin, J.; Zhang, J.; Wu, R.; Qiao, L.; Fang, W.; Lu, T.; Cheng, Y.. Fabrication of high quality factor lithium niobate double-disk using a femtosecond laser. *Int. J. Optomechatronics* **2017**, *11*(1), 47-54.

13 Chiles, J.; Buckley, S.; Nader, N.; Nam, S.W.; Mirin, R.P.; Shainline, J.M. Multi-planar amorphous silicon photonics with compact interplanar couplers, cross talk mitigation, and low crossing loss. *APL Photonics* **2017**, *2*(11), 116101.

14 Deubel, M.; Von Freymann, G.; Wegener, M.; Pereira, S.; Busch, K.; Soukoulis, C.M. Direct laser writing of three-dimensional photonic-crystal templates for telecommunications. *Nat. Mater.* **2004**, *3*(7), 444.

15 Sakellari, I.; Yin, X.; Nesterov, M.L.; Terzaki, K.; Xomalis, A.; Farsari, M. 3D Chiral Plasmonic Metamaterials Fabricated by Direct Laser Writing: The Twisted Omega Particle. *Adv. Opt. Mater.* **2017**, *5*(16).
16 Richter, B.; Hahn, V.; Bertels, S.; Claus, T.K.; Wegener, M.; Delaittre, G.; Barner-Kowollik, C.; Bastmeyer, M. Guiding cell attachment in 3D microscaffolds selectively functionalized with two distinct adhesion proteins. *Adv. Mater.* **2017**, *29*(5).
17 Li, Y.; Fang, Y.; Wang, J.; Wang, L.; Tang, S.; Jiang, C.; Zheng, L.; Mei, Y. Integrative optofluidic microcavity with tubular channels and coupled waveguides via two-photon polymerization. *Lab on a Chip* **2016**, *16*(22), 4406-4414.
18 Bückmann, T.; Thiel, M.; Kadic, M.; Schittny, R.; Wegener, M. An elasto-mechanical unfeelability cloak made of pentamode metamaterials. *Nat. Commun.* **2014**, *5*, 4130.
19 Schumann, M.; Bückmann, T.; Gruhler, N.; Wegener, M.; Pernice, W. Hybrid 2D–3D optical devices for integrated optics by direct laser writing. *Light Sci. Appl.* **2014**, *3*(6), e175.
20 Grossmann, T.; Schleede, S.; Hauser, M.; Beck, T.; Thiel, M.; von Freymann, G.; Mappes, T.; Kalt, H. Direct laser writing for active and passive high-Q polymer microdisks on silicon. *Opt. Express* **2011**, *19*(12), 11451-11456.
21 Siegle, T.; Schierle, S.; Kraemmer, S.; Richter, B.; Wondimu, S.F.; Schuch, P.; Koos, C.; Kalt, H. Photonic molecules with a tunable inter-cavity gap. *Light Sci. Appl.* **2017**, *6*(3), e16224.
21A Girault, P.; Lorrain, N.; Poffo, L.; Guendouz, M.; Lemaitre, J.; Carré, C.; Gadonna, M.; Bosc, D.; Vignaud, G. Integrated polymer micro-ring resonators for optical sensing applications. *J. Appl. Phys.* **2015**, *117*(10), 104504.
22 Klein, F.; Richter, B.; Striebel, T.; Franz, C.M.; Freymann, G.V.; Wegener, M.; Bastmeyer, M. Two-component polymer scaffolds for controlled three-dimensional cell culture. *Adv. Mater.* **2011**, *23*(11), 1341-1345.
22A Li, L.; Lin, H.; Qiao, S.; Huang, Y.Z.; Li, J.Y.; Michon, J.; Gu, T.; Alosno-Ramos, C.; Vivien, L.; Yadav, A.; Richardson, K. Monolithically integrated stretchable photonics. *Light Sci. Appl.* **2018**, *7*(2), 17138.
22B Chen, Y.; Li, H.; Li, M. Flexible and tunable silicon photonic circuits on plastic substrates. *Sci. Rep.* **2012**, *2*, 622.
23 White T. J; Broer D. J. *Nat. Mater.* **2015**, *14*(11), 1087.
24 Yamada M.; Kondo M.; Miyasato R.; Naka Y.; Mamiya J.; Kinoshita M.; Shishido A.; Yu Y.; Barrett C. J.; Ikeda T.*J. Mater. Chem.* **2009**, 19 (1), 60.
25 Zeng, H.; Wasylczyk, P.; Parmeggiani, C.; Martella, D.; Burresi, M.; Wiersma, D.S. Light-Fueled Microscopic Walkers. *Adv. Mater.* **2015**, *27*(26), 3883-3887.
26 Camacho-Lopez, M.; Finkelmann, H.; Palffy-Muhoray, P.; Shelley, M. Fast liquid-crystal elastomer swims into the dark. *Nat. Mater.* **2004**, *3*(5), 307.
27 Xu Q.; Schmidt B. Pradhan, S., Lipson, M. Micrometre-scale silicon electro-optic modulator. *Nature* **2005**, *435*(7040), 325.
27A Dong, P.; Liao, S.; Feng, D.; Liang, H.; Zheng, D.; Shafiiha, R.; Kung, C.C.; Qian, W.; Li, G.; Zheng, X.; Krishnamoorthy, A.V. Low V pp, ultralow-energy, compact, high-speed silicon electro-optic modulator. *Opt. Express* **2009**, *17*(25), 22484-22490.
28 Armani, D.; Min, B.; Martin, A.; Vahala, K. J. Electrical thermo-optic tuning of ultrahigh-Q microtoroid resonators. *Appl. Phys. Lett.* **2004**, *85*(22), 5439.

28A Nawrocka, M.S.; Liu, T.; Wang, X.; Panepucci, R.R. Tunable silicon microring resonator with wide free spectral range. *Appl. Phys. Lett.* **2006**, *89*(7), 071110.
28B Sun, C.; Wade, M.T.; Lee, Y.; Orcutt, J.S.; Alloatti, L.; Georgas, M.S.; Waterman, A.S.; Shainline, J.M.; Avizienis, R.R.; Lin, S.; Moss, B.R. Single-chip microprocessor that communicates directly using light. *Nature* **2015**, *528*(7583), 534.
28C Dong, P.; Qian, W.; Liang, H.; Shafiiha, R.; Feng, D.; Li, G.; Cunningham, J.E.; Krishnamoorthy, A.V.; Asghari, M. Thermally tunable silicon racetrack resonators with ultralow tuning power. *Opt. Express* **2010**, *18*(19), 20298-20304.
28D Dong, P.; Qian, W.; Liang, H.; Shafiiha, R.; Feng, N.N.; Feng, D.; Zheng, X.; Krishnamoorthy, A.V.; Asghari, M. Low power and compact reconfigurable multiplexing devices based on silicon microring resonators. *Opt. Express* **2010**, *18*(10), 9852-9858.
29 Almeida, V. R.; Barrios, C. A.; Panepucci, R. R.; Lipson, M. All-optical control of light on a silicon chip. *Nature* **2004**, *431*(7012), 1081.
30 Wang, C. T.; Tseng, C. W.; Yu, J. H.;, Li, Y.C.; Lee, C.H.; Jau, H. C.; Lee, M. C.; Chen, Y.J.; Lin, T.H. Optical bistability in a silicon nitride microring resonator with azo dye-doped liquid crystal as cladding material. *Opt. Express*, **2013**, 21,10989-10994.
31 Muller, N.; Haberko, J.; Marichy, C.; Scheffold, F. Photonic hyperuniform networks obtained by silicon double inversion of polymer templates. *Optica* **2017**, *4*(3), 361-366.
32 Maire, G.; Vivien, L.; Sattler, G.; Kaźmierczak, A.; Sanchez, B.; Gylfason, K.B.; Griol, A.; Marris-Morini, D.; Cassan, E.; Giannone, D.; Sohlström, H. High efficiency silicon nitride surface grating couplers. *Opt. Express* **2008**, *16*(1), 328-333.
33 Chen, X.; Li, C.; Fung, C.K.; Lo, S.M.; Tsang, H.K.. Apodized waveguide grating couplers for efficient coupling to optical fibers. *IEEE Photon. Technol. Lett.* **2010**, *22*(15), 1156-1158.
34 Van Laere, F.; Roelkens, G.; Ayre, M.; Schrauwen, J.; Taillaert, D.; Van Thourhout, D.; Krauss, T.F.; Baets, R. Compact and highly efficient grating couplers between optical fiber and nanophotonic waveguides. *J. Light. Technol.* **2007**, *25*(1), 151-156.
35 Selvaraja, S.K.; Vermeulen, D.; Schaekers, M.; Sleeckx, E.; Bogaerts, W.; Roelkens, G.; Dumon, P.; Van Thourhout, D.; Baets, R. Highly efficient grating coupler between optical fiber and silicon photonic circuit. *Conference on Lasers and Electro-Optics* **2009**, CTuC6
36 Zhang, H.; Li, C.; Tu, X.; Song, J.; Zhou, H.; Luo, X.; Huang, Y.; Yu, M.; Lo, G.Q. Efficient silicon nitride grating coupler with distributed Bragg reflectors. *Opt. Express* **2014**, *22*(18), 21800-21805.
36A Landowski, A.; Zepp, D.; Wingerter, S.; von Freymann, G.; Widera, A.; Direct laser written polymer waveguides with out of plane couplers for optical chips. *APL Photonics* **2017**, *2*(10), 106102.
36B Lindenmann, N.; Balthasar, G.; Hillerkuss, D.; Schmogrow, R.; Jordan, M.; Leuthold, J.; Freude, W.; Koos, C. Photonic wire bonding: a novel concept for chip-scale interconnects. *Opt. Express* **2012**, *20*(16), 17667-17677.
36C Wong, W.H.; Zhou, J.; Pun, E.Y.B. Low-loss polymeric optical waveguides using electron-beam direct writing. *Appl. Phys. Lett.* **2001**, *78*(15), 2110-2112.
37 Righini, G.C.; Dumeige, Y.; Féron, P.; Ferrari, M.; Nunzi Conti, G.; Ristic, D.; Soria, S.. Whispering gallery mode microresonators: fundamentals and applications. *Rivista del Nuovo Cimento* **2011**, *34*(7), 435-488.

38 Gaso, P.; Jandura, D.; Pudis, D.; Lettrichová, I. 3D ring resonator prepared by laser lithography embedded in PDMS. *Integrated Photonics: Materials, Devices, and Applications IV* **2017,** 10249, 102490C
39 Ramiro-Manzano, F.; Prtljaga, N.; Pavesi, L.; Pucker, G.; Ghulinyan, M.. A fully integrated high-Q whispering-gallery wedge resonator. *Opt. Express* **2012**, *20*(20), 22934-22942.
40 Ghulinyan, M.; Ramiro-Manzano, F.; Prtljaga, N.; Guider, R.; Carusotto, I.; Pitanti, A.; Pucker, G.; Pavesi, L. Oscillatory vertical coupling between a whispering-gallery resonator and a bus waveguide. *Phys. Rev. Lett.* **2013**, *110*(16), 163901.
41 Ghulinyan, M.; Guider, R.; Pucker, G.; Pavesi, L. Monolithic whispering-gallery mode resonators with vertically coupled integrated bus waveguides. *PTL. IEEE Photon. Technol. Lett.* **2011**, *23*(16), 1166-1168.
42 Warner, M.; Terentjev, E. Liquid Crystal Elastomers. Oxford Univ **2007**.
43 Broer, D.; Crawford, G.P.; Zumer, S. Cross-linked liquid crystalline systems: from rigid polymer networks to elastomers. CRC press **2011**.
44 Zeng, H.; Wasylczyk, P.; Cerretti, G.; Martella, D.; Parmeggiani, C.; Wiersma, D.S. Alignment engineering in liquid crystalline elastomers: Free-form microstructures with multiple functionalities. *Appl. Phys. Lett.* **2015**, *106*(11), 111902.
45 Martella, D.; Antonioli, D.; Nocentini, S.; Wiersma, D.S.; Galli, G.; Laus, M.; Parmeggiani, C. Light activated non-reciprocal motion in liquid crystalline networks by designed microactuator architecture. *RSC Advances* **2017**, *7*(32), 19940-19947.
46 Zeng, H.; Martella, D.; Wasylczyk, P.; Cerretti, G.; Lavocat, J.C.G.: Ho, C.H.; Parmeggiani, C.; Wiersma, D.S. High-resolution 3D direct laser writing for liquid-crystalline elastomer microstructures. *Adv. Mater.* **2014**, *26*(15), 2319-2322.
47 Flatae, A.M.; Burresi, M.; Zeng, H.; Nocentini, S.; Wiegele, S.; Parmeggiani, C.; Kalt, H.; Wiersma, D. Optically controlled elastic microcavities. *Light Sci. Appl.* **2015**, *4*(4), e282.
48 Liu, D.; Broer, D.J. Liquid crystal polymer networks: preparation, properties, and applications of films with patterned molecular alignment. *Langmuir* **2014**, *30*(45), 13499-13509.
49 Gissibl, T.; Wagner, S.; Sykora, J.; Schmid, M.; Giessen, H. Refractive index measurements of photo-resists for three-dimensional direct laser writing. *Opt. Mater. Express* **2017**, *7*(7), 2293-2298.